Macromolecules

pubs.acs.org/Macromolecules Article

Effects of Chain Length on the Structure and Dynamics of Semidilute Nanoparticle–Polymer Composites

Ari Y. Liu, Hamed Emamy, Jack F. Douglas, and Francis W. Starr*

Cite This: *Macromolecules* 2021, 54, 3041–3051 Read Online

ACCESS | Metrics & More | Article Recommendations | Supporting Information

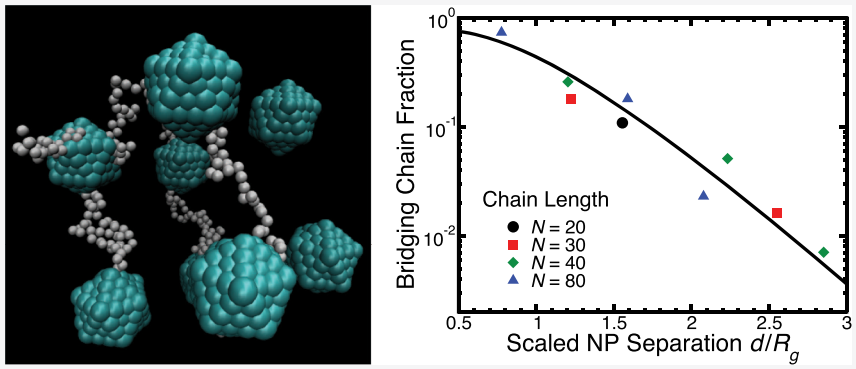

ABSTRACT: We use molecular dynamics simulations to study how the chain length affects the structure and segmental dynamics of polymer–nanoparticle (NP) composites at semidilute NP concentrations. For NPs having relatively strong interactions with the polymer, we can approximate the system as an ideal NP dispersion, which isolates the effect of direct interactions among the NPs. By varying both the chain length N and NP concentration, we examine regimes where the chain size (i.e., chain radius of gyration R_g) is small compared to the NP separation d ($d/R_g > 1$), as well as cases where $d/R_g < 1$, so that chains readily "bridge" between the NPs. We find that the fraction of such bridging chains in our simulations can be expressed as a universal function of d/R_g. Structurally, the polymers slightly elongate near the NP interface and the chains tend to align their longest axis with the NP interface. We show that the effect of NPs on the chain structure is nearly chain length-independent, whereas the effect on chain alignment extends farther from the NP surface as the chain length increases. Chains that bridge between NPs must significantly elongate when the NP separation is large compared to the chain dimensions ($d/R_g > 1$). Although these bridging chains have a longer relaxation time than nonbridging chains, they do not make a substantial contribution to the overall nanocomposite segmental relaxation time for the conditions studied because the bridging chains represent only a small fraction of the system. Note that relaxation at the scale of chains may differ for bridging chains. When NP separation is comparable or smaller than the chain size ($d/R_g < 1$), bridging chains are more prevalent, but their properties are more similar to nonbridging chains than when $d/R_g > 1$. Accordingly, the variation of the computational glass transition temperature T_g with chain length essentially mirrors the trend for the reference pure polymer melt, where T_g increases with chain length and roughly saturates at large polymer mass. Overall, for the conditions studied, bridging chains are found to have a small impact on the segmental dynamics of nanocomposites.

1. INTRODUCTION

The addition of fillers to polymers has long been used to modify material properties, and thus, understanding the interactions in polymer composites is important for developing novel materials of this kind. Compared to larger-scale filler particles, nanoparticles (NPs) have a higher surface-to-volume ratio and thus yield a larger volume of interfacial polymer matrix, so that even a small concentration of NP additives can create appreciable changes to the dynamical, mechanical, optical, and electrical properties of materials.[1−18] The processing of these materials commonly occurs in the amorphous melt state above the glass transition temperature T_g so that the effect of NP additives on T_g plays an essential role in both mechanical properties and practical manufacturing concerns. It is already well-appreciated that attractive interactions between polymers and NPs favor NP dispersion and tend to slow the dynamics of the interfacial polymer, thus increasing the overall T_g of the material.[13,19−27] On the other hand, strong polymer–NP interactions do not necessarily lead to large increases in T_g. This seemingly paradoxical situation

Received: November 7, 2020
Revised: February 9, 2021
Published: March 23, 2021

https://doi.org/10.1021/acs.macromol.0c02500
Macromolecules 2021, 54, 3041–3051

has been attributed to the formation of a "bound" polymer layer having a substantially slower polymer interfacial dynamics.[25,28−32] The bound layer effectively decouples from the surrounding polymer matrix and shields the matrix from NP influence when the separation between NPs is larger than the scale of the bound region. As a consequence, the shift of T_g saturates for a highly attractive particle−polymer interaction strength.[28−31,33] We caution here that the strong attraction can drive the interfacial layer around the NP into a nonequilibrium state in which quasi-thermodynamic measurements (such as specific heat or thermal expansion) become insensitive to the very slow relaxation of the interfacial region between the NP and the surrounding polymer matrix. In other words, the interfacial layer is thermodynamically "dead" so that the slow dynamics do not register in these "quasi-dynamic" measurements.[34]

In addition to interfacial effects on composite dynamics, it has been argued that "bridging" chains between the NPs (i.e., chains that are in contact with at least two different NPs) may also substantially alter the composite properties. In this conception of the effects of NPs on the material, there are at least three regimes:[32] (i) the dilute limit, where changes are due entirely to interfacial effects; (ii) the high concentration limit, where interfacial regions overlap, which can also lead to polymer confinement effects; and (iii) a "semidilute" regime where interfacial regions are distinct, but possibly linked by chains bridging between the NPs. Previous work has focused mainly on the dilute NP regime,[19,20,22,32,35] and other studies have demonstrated that interaction between interfacial chains at large NP concentrations can enhance the mechanical and dynamical properties of materials.[36−42] In this high NP concentration regime, the interfacial zones of the isolated particles studied before can overlap, forming a percolating network of the interfacially connected regions in which the dynamics are greatly influenced by the NPs, ultimately leading to significant mechanical reinforcement.[38,39] Here, we wish to examine the case of semidilute concentration, where the NPs are still well-dispersed and the interfacial layers do not percolate, but where longer chains can potentially bridge between different NPs. In the current paper, we use molecular dynamics simulations to examine to what extent bridging occurs in an ideal dispersion of NPs in this regime with strongly attractive polymer−NP interactions, and how bridging alters the chain structure and the resulting composite dynamics. The degree of such bridging is affected by both the NP spacing and chain length. Accordingly, we examine both the variable chain length and NP concentration (which alters NP separation).

The results of our simulations indicate that, in the semidilute concentration range in which the NPs are well dispersed and their interfacial zones do not strongly overlap, the fraction of bridging chains is a universal function of the ratio of NP separation and chain size. Bridging chains between NPs can have significantly altered conformations and segmental relaxation times, in comparison to nonbridging chains. In particular, the bridging chains tend to be extended along the direction connecting between the NPs, and dynamically, the bridging chains have a longer relaxation time compared to the nonbridging chains. However, the structural and dynamical differences of the bridging chains (compared to the mean) are only significant when the NP separation becomes comparable or larger than the chain radius of gyration. In the semidilute concentration that we study, the fraction of such bridging chains is small, and consequently, their effect on the overall properties of the composite is minimal. We also find that the chain length N does not have a significant impact on the chain structure at the NP interface, as found before for chains at planar[43] interfaces, but NP interfacial effects on chain alignment extend farther from the NP surface as N increases. Regarding the dynamics of composites, we find that the relative changes in T_g with N track those of the pure polymer melt. Of course, the polymer−NP composites shift T_g in their own right, but this shift (relative to the pure melt) is not sensitive to polymer mass over the range we study; it is a relatively local effect derived from the impact of the NPs on the polymer interfacial zone surrounding the particles, as addressed in previous studies of the "infinitely dilute" limit.[44,45] For pure melts, previous experiments and simulations have shown that T_g increases and roughly saturates with N. More precisely, changes in T_g approximately follow a linear relationship with $1/N$.[46−51] We find the same effect of chain length on the T_g in our model polymer−NP composites, independent of the concentration of the NP and unaffected by the presence of bridging chains. In short, we only find a significant difference in the properties of bridging chains under the circumstances in which they must stretch a large distance between NPs, but in such cases, bridging chains are rare. As a result, chain bridging does not have a significant impact on the overall structure and dynamics of composites in the semidilute concentration regime when the NPs are well dispersed. Our findings are specific to the case of static well-dispersed NPs, and bridging may have a different effect when NPs dynamically aggregate and diffuse, an area for future investigation.

2. METHODS

We model the polymer composites as an ideal, uniform dispersion of NPs surrounded by the polymer melt; further details about the nanocomposite model can be found in earlier studies.[19,31,32] All simulations are performed using LAMMPS;[52] the Kremer−Grest bead-spring model is used to model the polymer chains, which are composed of 5−80 monomers in order to evaluate chain length effects. Nonbonded monomers interact via a Lennard-Jones (LJ) potential truncated and shifted at $r_c = 2.5\sigma$ such that it includes attraction, where σ is the diameter of the LJ potential. Bonded monomers in a chain are connected by a finitely extensible nonlinear elastic potential (FENE), with the bond strength $k_0 = 30$. Each NP consists of 104 beads (identical to the monomers of polymer chains) to form an icosahedron of edge length $a = 4.4\sigma$ (4 monomers per edge) corresponding to a diameter $d = 6.6\sigma$ for the inscribed sphere. The NPs and polymers interact via an attractive LJ interaction of strength $\epsilon_{p-NP} = 1.5\epsilon$ (ϵ is the polymer−polymer interaction strength), also truncated at $r_c = 2.5\sigma$. We choose a relatively attractive polymer−NP interaction strength that would correspond to good dispersion of NPs and potentially will be favorable for bridging interactions. We define the NP concentration $\phi = N_{NP}/(N_{NP} + N_{poly})$ (which roughly equals the volume fraction), where N_{NP} is the number of NP force sites and N_{poly} is the number of polymer monomers. We simulate composites with three different NP concentrations (ϕ = 2.8, 5.5, and 10.4%) by varying the total number of polymer chains. For each NP concentration, we study seven different chain lengths N = 5, 10, 15, 20, 30, 40, and 80 of the polymers, each case corresponding to a different total number of chains in the composite. For relatively short polymer chains (here, $N \leq 20$ in ϕ = 2.8% and 5.5% and $N \leq 15$ in ϕ = 10.4%), a single NP is fixed at the center of the simulation box and surrounded by polymers (Figure 1a) with a total number of monomers N_{poly} = 3600, 1800, and 900, corresponding to ϕ = 2.8, 5.5, and 10.4%; by periodic boundary conditions, this single NP mimics an ideal dispersion of the NP. For longer chains or higher concentrations (here, when $N \geq 30$ in ϕ = 2.8 and 5.5% and $N \geq 20$ in ϕ = 10.4%),

https://doi.org/10.1021/acs.macromol.0c02500
Macromolecules 2021, 54, 3041−3051

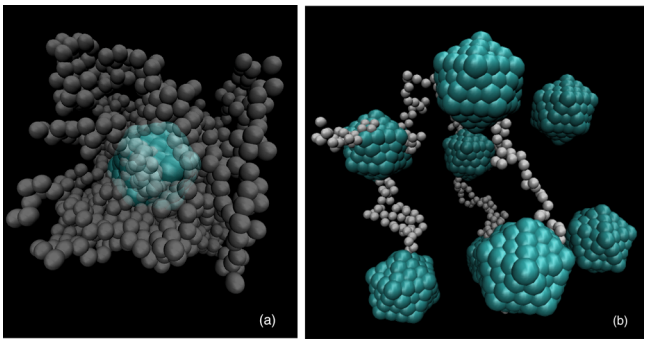

Figure 1. (a) A "snapshot" from our simulations, in which we have a NP fixed at the center of a simulation box and surrounded by polymer melts. We only show some of the chains here for clarity. (b) To avoid the potential finite size effect when studying longer chains, we set up simulations with eight NPs in a correspondingly larger simulation box. This image shows some of the chains that bridge between the NPs.

we use a larger simulation cell with eight fixed NPs surrounded by eight times the number of polymer chains as compared to the single NP systems (Figure 1b). Accordingly, the total number of monomers is N = 28, 800, 14,400, and 7200 for the three concentrations ϕ = 2.8%, 5.5%, and 10.4%, respectively. These larger simulations ensure that the simulation cell size is always more than double the largest dimension of the chain (defined by the eigenvalues of the radius of gyration tensor) so that we avoid potential finite-size effects. Simulations are performed in an NVT ensemble along an isobaric path with pressure P = 0.1 and temperatures ranging from 0.42 to 0.80, in reduced LJ units $T^* = k_BT/\epsilon$, where ϵ is the polymer–polymer interaction strength and k_B is the Boltzmann constant. All results are reported in reduced units of the monomer diameter σ and interaction strength ϵ that can be approximately converted to real units for a typical polymer-like polystyrene with $T_g \approx 100$ °C by choosing $\sigma \approx 2$ nm, $\epsilon \approx 10$ kJ/mol, $m \approx 0.5$ kg/mol, and one time unit ≈15 ps. Using this mapping, the lowest simulated temperature $T \approx 200$ °C, which is higher than the experimental T_g due to the inherent limitations on the longest time scales accessible to simulation. The chain lengths simulated (N = 5 to 80 monomers) can be mapped to molecular weights ≈2.5 kg/mol to 20 kg/mol, the cutoff of LJ potential $r_c \approx 5$ nm, and the approximate diameter of NP $d \approx 12$ nm.

3. CHAIN STRUCTURE AND ORIENTATION IN POLYMER–NP COMPOSITES

In this section, we examine the chain length effects on the orientation and chain dimensions of polymers. Previous work has shown that interaction of chains with the NP can lead to an expansion and alignment of polymers near the NP interface.[53−60] We show below that such changes to the chain structure are largely independent of the chain length N, whereas changes in the chain orientation do exhibit a chain length dependence. We will also evaluate the structural and orientational properties of bridging chains and show that they behave differently from a typical chain in the polymer matrix; that said, the bridging chains have only a modest impact on the overall structural properties.

3.1. Overall Chain Structure and Orientation with Respect to the NP Surface. We first examine the chain length effect on the overall structural and orientational properties of polymers. To characterize the structure of polymer chains, we study the gyration tensor

$$S_{\alpha\beta} = \frac{1}{N}\sum_{i=1}^{N}(r_i^{\alpha} - r_{cm}^{\alpha})(r_i^{\beta} - r_{cm}^{\beta}) \quad (1)$$

where N denotes the chain length, r_i^{α} is the position of monomer i within the chain in the α direction, and r_{cm} is the center of mass (COM) of the chain. The eigenvalues (λ_i^2, with the convention $\lambda_1^2 < \lambda_2^2 < \lambda_3^2$) of this tensor are evaluated to

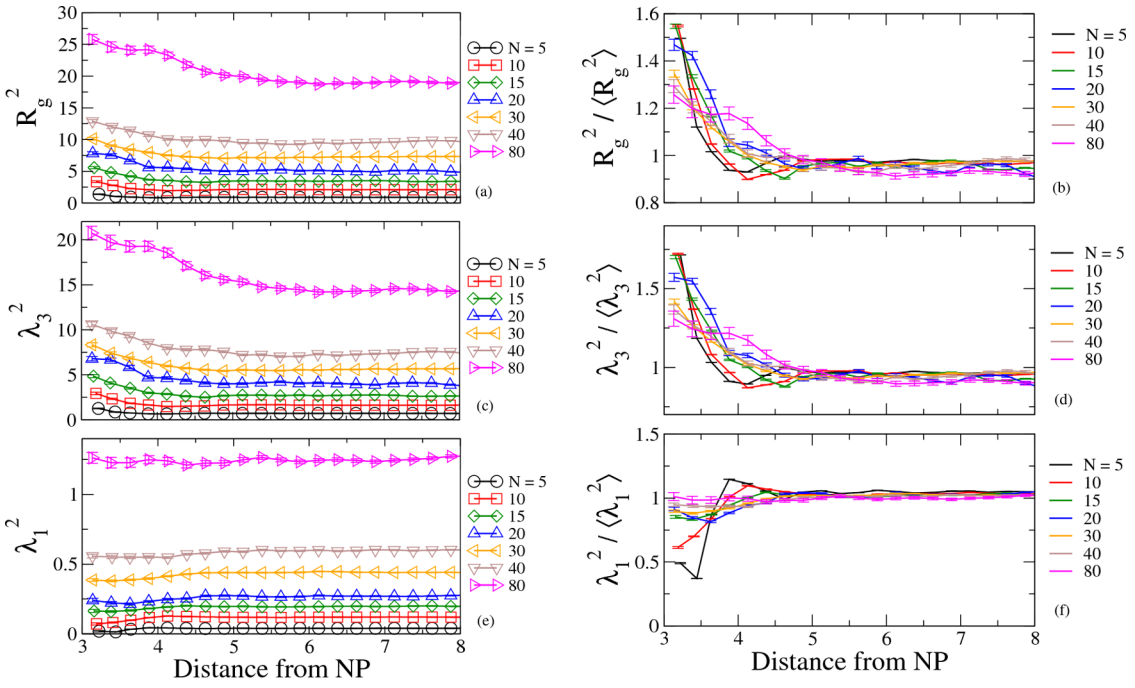

Figure 2. NP effects on chain dimensions. We show data from 2.8% NP simulations here as an example. Since the chain dimension is not affected by temperature, data are averaged over T. (a) Radius of gyration R_g^2 and (b) when scaled by its average value show that R_g^2 increases for chains approaching the NP surface, independent of the chain length. (c,d) Largest eigenvalue of the gyration tensor λ_3^2 increases near the NP surface. (e,f) Smallest eigenvalue λ_1^2 decreases near the NP surface.

https://doi.org/10.1021/acs.macromol.0c02500
Macromolecules 2021, 54, 3041−3051

quantify the shape of polymers. We also define the overall radius of gyration by summing the eigenvalues, $R_g^2 = \sum_i \lambda_i^2$. Figure 2 summarizes the shape variations in terms of R_g^2 and the largest (λ_3^2) and smallest eigenvalues (λ_1^2) from simulations with ϕ = 2.8%, as a function of distance from the NP center to the chain COM. Figure 2a shows that the radius of gyration R_g^2 increases for chains approaching the NP surface. To eliminate trivial chain length effects from these data, we scale $R_g^2(N)$ by the corresponding average value $\langle R_g^2(N)\rangle$ for each chain length; this scaling demonstrates that the normalized R_g^2 is *independent* of chain length, consistent with previous studies.[19,61] Similar to R_g^2, we show the largest λ_3^2 and smallest λ_1^2 eigenvalues of the gyration tensor in Figure 2c,e, respectively, as well as the values normalized by the corresponding average values in Figure 2d,f. These data show that λ_3^2 increases near the NP surface (like R_g^2), while λ_1^2 *decreases* near the NP surface, an effect that is more prominent for shorter chains, and nearly disappears at the longest chain length N = 80. Thus, the overall expansion of the chains can be attributed to the extension along the long axis of the polymer. Since the smallest axis simultaneously decreases, the chains qualitatively change shape from something more egg-shaped to something more akin to a cigar. The plot for λ_3^2 normalized by the average (Figure 2d) shows that the NP interfacial effects on the long axis are nearly independent of chain length. The interfacial changes extend slightly farther from the NP surface for the longest chains. Meanwhile, Figure 2f of λ_1^2 normalized by its average shows that the changes along the shortest axis are nonuniversal near the NP surface, as the changes are larger for the shorter chains. However, the nonuniversal behavior of λ_1^2 does not significantly affect the overall R_g^2 behavior, which is naturally dominated by the largest eigenvalue λ_3^2.

The packing of polymers on the NP surface also causes changes to the orientation of chains. We evaluate the orientational order parameter defined by the second Legendre polynomial

$$\langle P_2(\cos\theta_i)\rangle = \frac{1}{2}\langle(3\cos^2\theta_i - 1)\rangle \quad (2)$$

where θ_i is the angle between the vector of chain COM relative to the NP center and the semiaxis eigenvector $\mathbf{e_i}$ of the gyration tensor, associated to eigenvalue λ_i^2. $P_2(\cos\theta_i) = -0.5$ if $\mathbf{e_i}$ is normal to the NP radial direction, and $P_2(\cos\theta_i) = 1$ when $\mathbf{e_i}$ is parallel to the radial direction. When chains are randomly oriented with respect to the NP center, $\langle P_2(\cos\theta_i)\rangle = 0$ when averaged. Figure 3 shows the orientation of the smallest $\mathbf{e_1}$ and largest $\mathbf{e_3}$ semiaxis, as a function of distance from the NP center to the chain COM. Far away from the NP, $\langle P_2(\cos\theta_i)\rangle \approx 0$ for all axes, and thus, polymers are oriented isotropically far from the NP surface. Approaching the NP surface, $\langle P_2(\cos\theta_1)\rangle$ increases while $\langle P_2(\cos\theta_3)\rangle$ decreases, demonstrating that chains tend to align their shortest axis normal to the NP surface (along the radial direction) and the longest axis along the NP surface. Comparing the orientational data across different chain lengths, we find that as the chain length increases, the orientational changes start to appear farther away from the NP surface and become slightly less prominent near the surface of the NP. In other words, the larger chain lengths have orientational effects that extend farther from the NP interface. Thus, even though the changes in chain dimension are nearly independent of the chain length, the changes in chain orientation approaching the NP surface are more sensitive to the chain length.

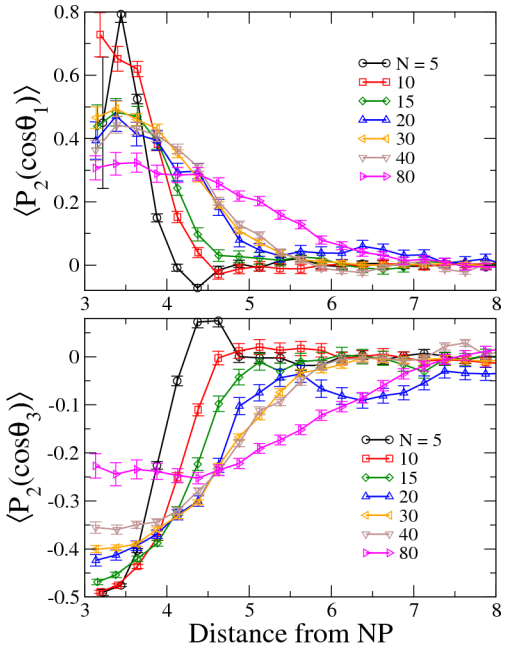

Figure 3. Chain alignment with the NP interface. We evaluate the orientational parameter (eq 2) for the eigenvectors $\mathbf{e_1}$ and $\mathbf{e_3}$ of the gyration tensor, corresponding to the smallest and largest semiaxis. The data show that the longest axis aligns parallel to the interface (normal to the NP radius), and the shortest axis aligns normal to the interface (parallel to the NP radius). In other words, chains tend to align their longest axis along the NP surface and the shortest axis normal to the surface. Comparing data of different chain lengths, we see that changes in both orientation parameters extend farther from the NP as the chain length increases.

3.2. Structure and Orientation of Bridging Chains.

We next examine how the polymer chains that "bridge" between NPs differ in their structural properties from the polymer matrix chains. These bridging effects can potentially become significant for long polymers ($N \geq 30$ in ϕ = 2.8% and 5.5% and $N \geq 20$ in ϕ = 10.4%), where the chain length becomes comparable to the distance between the NP interfaces. We first examine the degree to which bridging occurs in composites with different chain lengths and NP concentrations. We define a bridging chain as a chain with at least one monomer in contact with the interface of two separate NPs; NP contact is defined as a monomer closer than the first minimum (r = 4.05) in the monomer density profile (see Supporting Information, Figure S1). Figure 4a shows that the fraction of bridging chains increases when the ratio of the chain length to NP separation grows; this can be achieved with either increasing chain length or NP concentration (since increasing concentration reduces NP separation). At the smallest NP concentration ϕ = 2.8% (largest NP separation), we find nearly no bridging chains, even at the longest chain length N = 80; the maximum amount fraction of bridging chains reaches ≈70% at the highest concentration ϕ = 10.4% and longest chain length N = 80. For comparison, we also identify chains in contact with only one NP. The fraction of chains in contact with one NP generally increases with ϕ and the chain length (Figure 4b), with the exception of the longest chain length N = 80 at the highest concentration ϕ = 10.4%; in this case of long chains and relatively high concentration, the majority of chains are bridging chains, so fewer chains are in contact with just one NP. Note that the fraction of bridging and contacting chains is

https://doi.org/10.1021/acs.macromol.0c02500
Macromolecules 2021, 54, 3041−3051

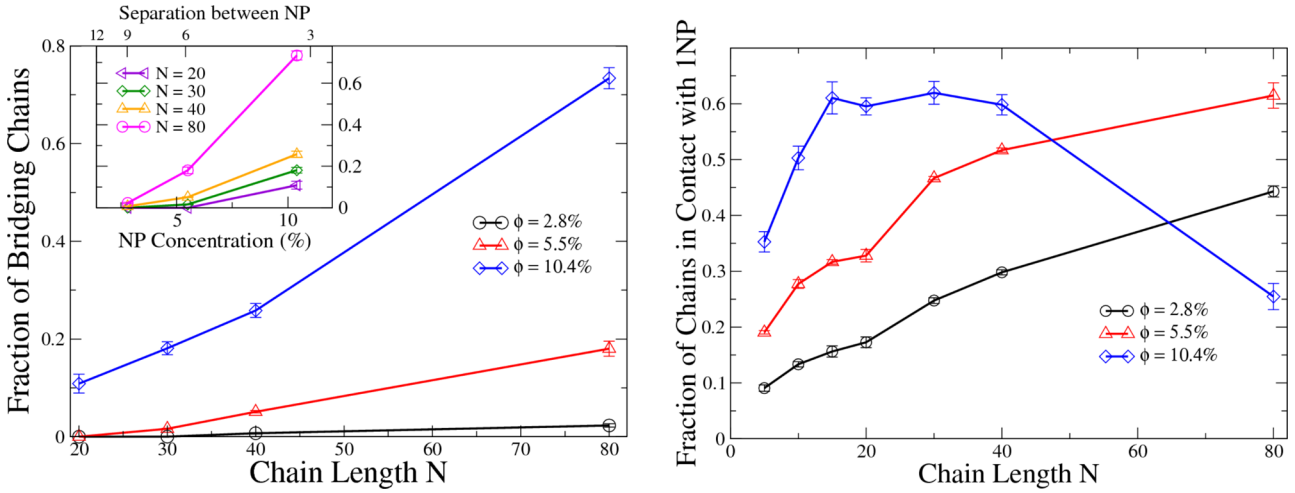

Figure 4. (a) Fraction of bridging chains as a function of chain length for each ϕ. The inset shows the fraction of bridging chains as a function of ϕ for each chain length. For systems with the highest NP concentration (ϕ = 10.4%), the separation between NPs is small enough that bridging starts to occur at chain length N = 20. (b) Fraction of chains in contact with only one NP (i.e., surface chains that do not bridge) generally increases with the chain length and concentration of the NP.

nearly independent of temperature, and thus, we show the data collected at T = 0.46 as an example.

Clearly, the fraction of bridging chains depends on the separation of the NP faces d (which directly relates to the NP concentration ϕ) and chain radius of gyration R_g (which directly relates to the chain length N). To quantify this relationship, we plot the fraction of bridging chains as a function of the ratio d/R_g for all chain lengths and concentrations for which bridging occurs (Figure 5).

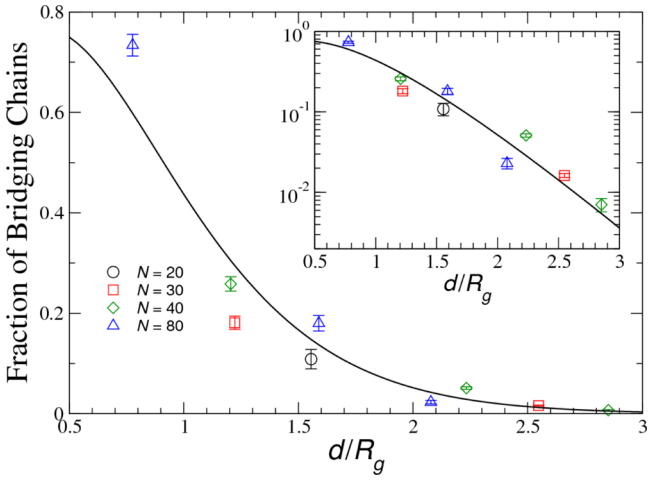

Figure 5. Fraction of bridging chains behaves as a universal function of d/R_g, and the inset shows that the functional dependence is approximately exponential with d/R_g. The line indicates the approximation $(1 + 6(d/R_g)^2)\exp[-2\sqrt{3}(d/R_g)]$, which follows from assuming chains are somewhat expanded compared to ideal Gaussian chains.

Apparently, the bridging fraction decreases exponentially with increasing d/R_g. This behavior can be understood by considering chain conformation and assuming that chains with $R_g > d$ bridge. If chains behaved ideally (where R_g follows a Gaussian distribution), the probability of bridging chains should vary like $(1 + \sqrt{6/\pi}(d/R_g))\exp[-3/2(d/R_g)^2]$ to the leading order in d/R_g. However, our chains are not ideal, and both excluded volume effects and interactions with the NP lead to chains that are expanded relative to the Gaussian model. If we assume that the radius of gyration follows a broader distribution proportional to $r^2 \exp[-\sqrt{12}(r/R_g)]$, we predict that the probability for bridging chains varies approximately as $(1 + 6(d/R_g)^2)\exp[-2\sqrt{3}(d/R_g)]$. This functional form describes our data to good approximation (line in Figure 5), so that we may understand the fraction of bridging chains from geometric considerations alone. We find that this bridging fraction is insensitive to temperature, further supporting the purely geometrical interpretation of the probability of chain bridging between NPs in a polymer melt. On the other hand, the chain residence time at the NP surrace is certainly temperature-dependent.

How do these bridging chains differ from other chains in structure and orientation? We evaluate the average radius of gyration $\langle R_{g,B}^2 \rangle$ and the orientational parameter $\langle P_{2,B}(\cos\theta_i) \rangle$ of the bridging chains to examine their structural properties (Figure 6). We find that bridging chains are (compared to the average) more elongated and tend to align the longest rotational axis normal to the NP surface and the shortest axis along the NP surface; in other words, bridging chains extend along the radial direction to connect between NPs. This property of bridging chains can be quantified by the observation that bridging chains have a larger $\langle R_{g,B}^2 \rangle$ and $\langle P_{2,B}(\cos\theta_3) \rangle$ (and smaller $\langle P_{2,B}(\cos\theta_1) \rangle$, not shown), compared to the average overall chains (and nonbridging chains, not shown). However, the differences in elongation and orientation are only significant at low NP concentration, where the separation between NPs is large compared to the chain dimension ($d > R_g$), so chains have to stretch out to bridge between different NPs. In these cases, the fraction of bridging chains is very low (≤1%). On the other hand, when there is a substantial amount of bridging chains at large concentration, the separation between NPs is comparable to R_g, so that the structure and orientation of bridging chains are not very different from other chains. Thus, when bridging chains have a significantly different structure, there are so few of them as to not strongly affect the average configuration over all polymer chains, and when there are many bridging chains, their

https://doi.org/10.1021/acs.macromol.0c02500
Macromolecules 2021, 54, 3041−3051

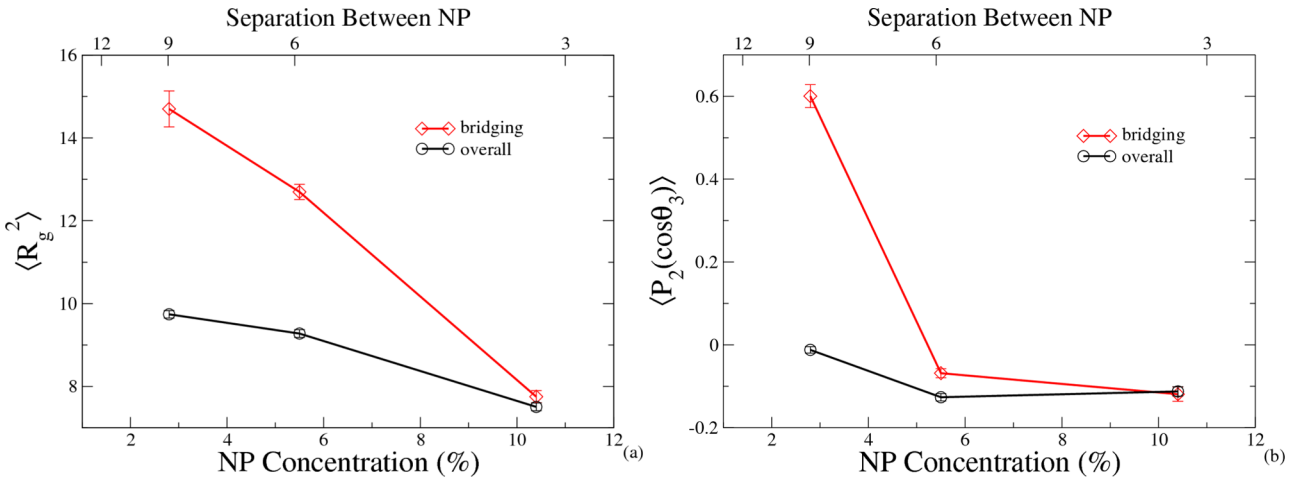

Figure 6. Structure and orientation of bridging chains compared to the overall: (a) R_g^2 averaged over the distance from NPs and (b) the orientational parameter associated with the longest rotational axis, averaged over the distance from NPs. We show the data from the example chain length $N = 40$, and the R_g^2 values convert to 15 nm to 30 nm in SI units. Bridging chains have relatively larger average $R_{g,B}^2$, and their longest axis, on average, aligns more perpendicular to the NP interface. However, the differences are significant only at low ϕ.

structure is close to that of the average. In either case, the average chain structure is not significantly altered. We also note that the chains in contact with only one NP show similar behavior to the average at all concentrations.

4. POLYMER DYNAMICS IN SEMIDILUTE POLYMER COMPOSITES

We next examine the sensitivity of dynamics and the nanocomposite glass transition to the chain length and the presence of bridging chains in the semidilute NP concentration regime of well-dispersed NPs. As discussed in the Introduction, it is well known that T_g increases and roughly saturates with increasing chain length.[49−51] Thus, we aim to examine the degree to which NPs and bridging chains modify (or not) the chain length dependence of dynamics of pure polymer melts. To quantify the composite dynamics, we calculate the self-intermediate scattering function

$$F_{self}(q, t) = \frac{1}{N}\left\langle \sum_{j=0}^{N} e^{iq\cdot(r_j(t)-r_j(0))} \right\rangle \quad (3)$$

where $r_j(t)$ is the position of monomer j at time t relative to a time origin and q is the scattering wave vector. Following convention, we examine $F_{self}(q, t)$ at the wave vector $q_0 = 7$, which is the approximate location of the primary peak in the monomer structure factor. Figure 7 shows the self-intermediate scattering function of composites with different chain lengths at representative $\phi = 2.8\%$ and $T = 0.46$; the data show that the segmental relaxation slows down as chain length increases (as expected from pure polymer materials) and saturates approaching the longest chains we study. This pattern is repeated across different NP concentrations and temperatures. We define the segmental relaxation time τ from the time at which when $F_{self}(q, \tau) = 1/e$. Reflecting the observed behavior of $F_{self}(q, t)$, the relaxation time τ (Figure 7 inset) increases with chain length and approaches saturation for the longest chain lengths.

To evaluate the effects of bridging on the dynamics, we compare the segmental relaxation of bridging chains with that of other chains. We calculate the self-intermediate scattering function and the corresponding segmental relaxation time τ for

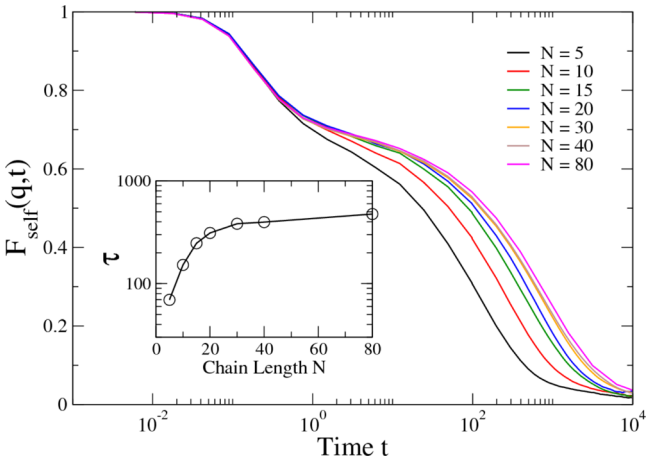

Figure 7. We evaluate the self-intermediate scattering function to extract the relaxation time τ (shown in the inset) for each system. Here, we show an example of $\phi = 2.8\%$ and $T = 0.46$ to demonstrate the chain length effect on polymer dynamics. Evidently, the relaxation becomes slower as the chain length increases. The glass transition temperature T_g (Figure 11a) itself follows a similar trend to τ shown in the inset. In physical units, the longest time scale in this figure probes to ≈150 ns, and τ ranges from ≈1 to ≈5 ns.

bridging chains (contacting two distinct NPs), chains in contact with just one NP, and their complements (nonbridging and noncontacting chains; see Supporting Information, Figure S5 for raw $F_{self}(q, t)$ data). Figure 8 shows the relaxation time τ from the simulations at $\phi = 5.5$ and 10.4%, where a substantial amount of bridging chains can be identified. Bridging chains clearly have a longer segmental relaxation time compared to nonbridging chains (consisting of both chains in contact with one NP and chains not in contact with any NP) and the average over all chains in the nanocomposite. Contacting chains also have relatively slower relaxation compared to the average but not as slow as the bridging chains. As the chain length increases (and the fraction of bridging chains increases, see Figure 4), the difference between τ of bridging chains and that of the average decreases. In other words, the dynamics of bridging chains only differ significantly when bridging between NPs requires the chains to be significantly expanded, as

https://doi.org/10.1021/acs.macromol.0c02500
Macromolecules 2021, 54, 3041−3051

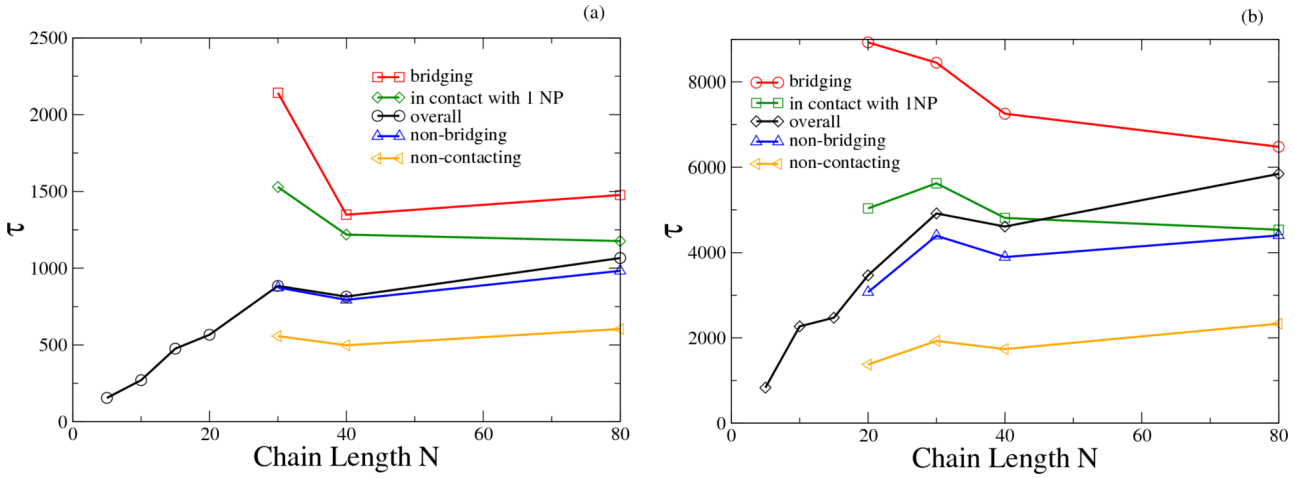

Figure 8. Segmental relaxation time τ for different types of chains in the (a) 5.5% NP composite and (b) 10.4% NP composite as a function of chain length, both at an example temperature $T = 0.46$. We show that bridging chains have slower relaxation compared to the average over all chains, nonbridging chains, chains that are in contact with one NP, and chains not in contact with the NP. In physical units, τ ranges from ≈2 ns to ≈30 ns for (a) $\phi = 5.5\%$ and ranges from ≈11 ns to ≈120 ns for (b) $\phi = 10.4\%$. In Figure. S6 in the Supporting Information, we plot the ratio $\tau_{bridging}/\tau_{overall}$.

described in the previous section. In this case, there are relatively few bridging chains so that their effect on the average segmental relaxation time is not significant. At a longer chain length, when there are a substantial number of bridging chains, their properties do not differ significantly from the averages, since the chains can bridge without significant changes in conformation. Consequently, the effects of bridging chains on the overall dynamics, both when there are few or many bridging chains, are minimal, similar to what we observed in the Chain Structure and Orientation in Polymer–NP Composites section.

We now consider if the chain length effects on dynamics differ as we change the NP concentration. We first examine the composite segmental relaxation time $\tau(T)$ normalized by the relaxation of pure polymers $\tau_{pure}(T)$ for each chain length and NP concentration (Figures 9 and 10). As expected, the relaxation is slower at larger NP concentrations. Figure 10 shows that τ follows a nearly logarithmic relationship with NP

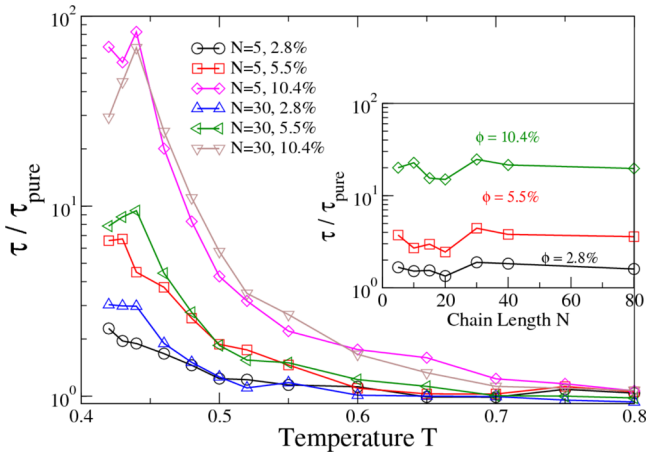

Figure 9. Segmental relaxation time τ of composites scaled by τ of pure polymer systems, as a function of temperature, plotted for the three different concentrations $\phi = 2.8\%$, 5.5%, and 10.4%. Only $N = 5$ and 30 are shown here as examples for each concentration. The inset shows τ/τ_{pure} as a function of N for each concentration at $T = 0.46$.

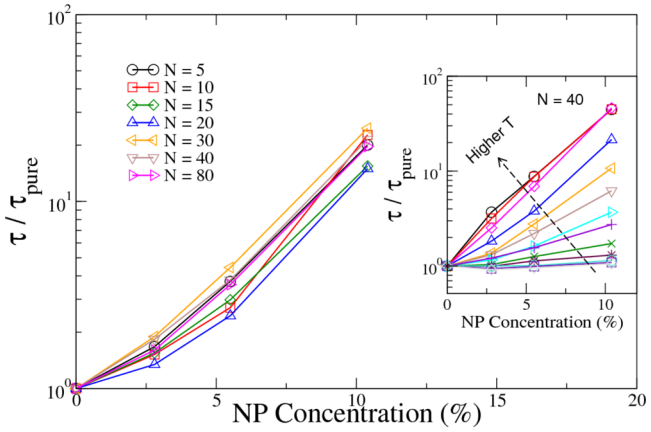

Figure 10. Scaled relaxation time τ/τ_{pure} of each chain length, plotted as a function of NP concentration ϕ at $T = 0.46$. The inset shows the composite τ/τ_{pure} at different temperatures for an example chain length $N = 40$. The change in slope with T depends on the polymer–NP interaction.[44] This type of variation of the relative change in relaxation time of NP-filled films with temperature has recently been observed experimentally.[62]

concentration ϕ for each chain length, and the inset shows that τ becomes more sensitive to temperature changes at higher NP concentrations. However, the chain length effect observed previously in $F_{self}(q, t)$ and τ disappears after scaling with $\tau_{pure}(T)$, indicating that dependence of the segmental relaxation time on the chain length stems solely from the chain length effect in the pure polymer system, since the influence of NPs on the composite dynamics is independent of the chain length in the cases studied,[44] and thus, bridging does not have a significant impact on the overall dynamics.

We also evaluate how the chain length and bridging influence the dynamical glass transition temperature T_g of composites. To facilitate estimation of T_g, we fit τ to the Vogel–Fulcher–Tammann (VFT) equation

$$\tau = \tau_0 \exp\left(\frac{DT_0}{T - T_0}\right) \quad (4)$$

https://doi.org/10.1021/acs.macromol.0c02500
Macromolecules 2021, 54, 3041–3051

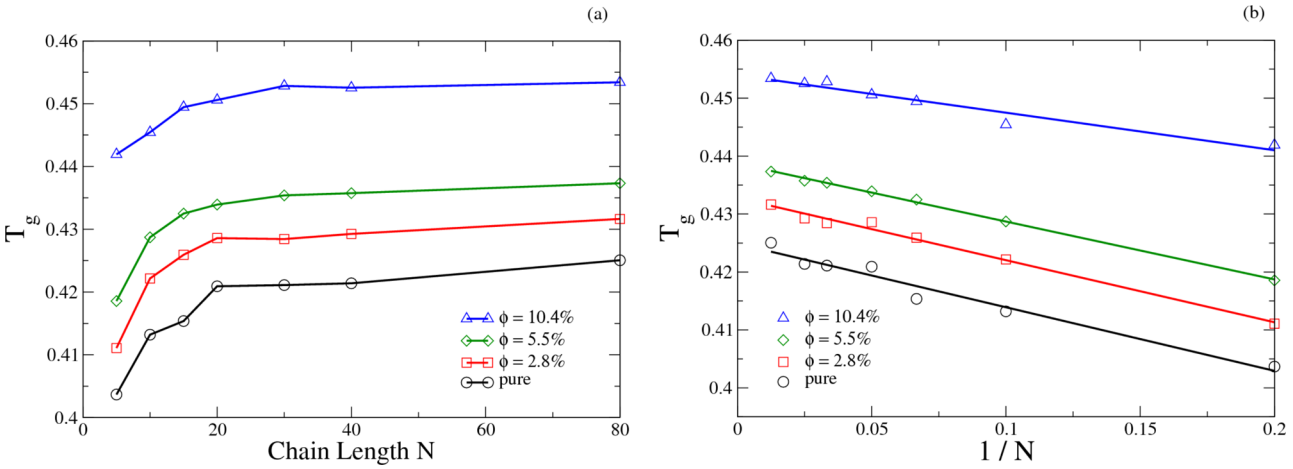

Figure 11. Glass transition temperature T_g of 2.8%, 5.5%, and 10.4% NP composites compared to that of the pure polymer system. The effect of the chain length on T_g remains consistent across different NP concentrations. (a) T_g as a function of chain length N. We show that the chain length effect in composite systems generally follows the trend in pure systems. (b) We show that $T_g(N = \infty) - T_g(N)$ has a linear relationship with $1/N$.

and define a dynamical T_g from the VFT fit when τ reaches 10,000 in LJ units (or ≈150 ns in lab units). This is a relatively short time scale from an experimental perspective; however, we avoid extrapolating the fit to experimental timescales, since the fit becomes unreliable when extrapolating more than a factor ≈10 beyond the largest τ value. We note that prior computational studies show that such a computational T_g has a roughly proportional variation to a T_g value obtained by extrapolating to experimental time scales on the order of 100 s.[31,63] Similar results can be obtained using alternate forms to fit τ. Figure 11a shows $T_g(N, \phi)$ plotted as a function of chain length for each NP concentration. Clearly, the computational T_g increases with ϕ, but the chain length dependence for all NP concentrations generally follows the trend in the pure polymer systems, where T_g grows with N and saturates at $N \approx 20$, consistent with previous experiments and simulations on pure polymer melts.[46−49] We also show that $T_g(N = \infty) - T_g(N)$ has an approximately linear relationship with $1/N$ (Figure 11b) regardless of NP concentration, as long-observed in pure polymer melts.[50,51,64−66] We can control the chain length effect in pure polymer systems by scaling $T_g(N, \phi)$ by $T_g(N)_{pure}$ (Figure 12); the scaled $T_g(N, \phi)/T_g(N)_{pure}$ shows no chain length dependence in the effect of concentration on T_g. This result demonstrates again that any chain length effect that we observe on the composite dynamics originates from the chain length effect already present in the pure systems. Also, since the segmental relaxation of bridging chains only differs from the overall relaxation significantly when the fraction of bridging is small, the dynamical T_g is not affected by bridging chains, a result in accordance with that on the overall chain structure.

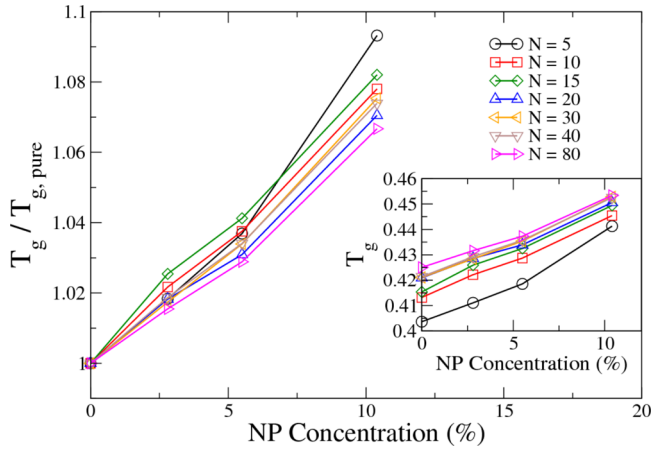

Figure 12. Glass transition temperature T_g of composites scaled by that of the pure systems with the corresponding chain lengths, as a function of NP concentration ϕ. We do not see significant chain length differences in the effect of concentration on T_g. The inset shows the composite T_g without scaling. Note that the sign of the change in T_g with NP concentration depends on the polymer−NP interaction: T_g increases with ϕ in our systems with relatively attractive polymer−NP interaction but T_g would decrease with ϕ for nonattractive interactions.[19,44]

5. CONCLUSIONS

We examined how the configurational and segmental relaxation properties of a polymer−NP composite are altered as we move from the dilute limit to a semidilute NP concentration range where chains start to bridge between NPs, but where the interfacial zones around the NP are not percolating. We find that the bridging chains can differ significantly from other chains under the conditions where they must elongate considerably to link the NPs. However, since the fraction of such bridging chains is small, their effect on the composite properties is correspondingly limited. When the chains are long enough to readily bridge between NPs without a substantial conformational change, their properties do not differ significantly from other chains, so we again see a minimal effect of bridging chains. Accordingly, the effect of the chain length on T_g of composites is not significantly affected by the presence of bridging chains, and the changes in T_g stem from the chain length effects found in pure polymer systems, where T_g increases and roughly saturates with the chain length. $T_g(N = \infty) - T_g(N)$ linearly decreases with $1/N$, which conforms with the long-established argument that the longer chain length leads to fewer free chain ends and lower free volume, thus resulting in a higher T_g.[50,51] Of course, as previously established in many studies, T_g can be substantially altered by varying the interaction strength between the polymers and NP.[19,20,22,25−27]

https://doi.org/10.1021/acs.macromol.0c02500
Macromolecules 2021, 54, 3041−3051

We also characterized the geometrical structure and dynamics of both bridging and nonbridging chains. Near the NP surface, the interfacial chains tend to elongate and align their longest axis along the NP surface. While the structural changes of the chain at the NP interface are nearly independent of the chain length, NP interfacial effects on chain alignment extend farther from the NP surface as the chain length increases. Bridging chains naturally tend to be extended along the direction connecting NPs and have slower relaxation compared to other chains, but, as noted above, the differences are only substantial when NP separation is large and the fraction of bridging chains is small. In general, the interfacial effects of the NP dominate the effects of bridging chains for all NP concentrations. When NP concentration is small and the distance between the NPs is large, bridging chains form with difficulty because of the high energetic cost of stretching. Ultimately, we conclude that bridging chains do not have significant effects on the properties of the segmental relaxation of NP composites in the semidilute concentration range we study, under the conditions that the polymer−NP interaction is relatively attractive so that the NPs remain well dispersed (as in the dilute limit). Future work should examine the role of bridging chains in the case where NPs can diffuse in the matrix and potentially aggregate, as bridging may have different effects in this case. In addition, the effect of bridging chains can differ at high NP concentration where the interfacial zone around the NPs starts to macroscopically percolate. We note that our conclusion that bridging chains play a minimal role in our polymer nanocomposite simulations does not extend to overall chain relaxation processes (as opposed to segmental relaxation) that involve the displacement of the polymer chains on the scale of their average size. Such relaxation processes are highly relevant to the polymer nanocomposite in the melt state, just as in the case of the neat polymer material. Such chain relaxation processes and the impact of polymer bridging may be studied at higher temperatures than the present study, where such a large scale displacement would be computationally accessible.

Although our results are "negative" in the sense that the often suggested hypothesis that chain bridging influences nanocomposite properties is not supported by our simulations, our results are, at the same time, highly "positive" in the sense that they support the applicability of our former nanocomposite model, in which changes in segmental dynamics were modeled by simply assuming a single NP in a box of varying size to capture concentration variation. To the leading order, this simplified model applies because each NP contributes nearly additively to the changes of the segmental dynamics. This finding suggests that we should be able to model NPs of complex shape and even extended NPs, by a similar "infinite dilution" polymer nanocomposite model, an approximation that makes such computations more tractable. Of course, this approach clearly has limitations as the concentrated NP regime is approached or if mobile NPs directly interact at low concentration. Model calculations in this concentration regime should be explored in the future.

■ ASSOCIATED CONTENT

Supporting Information

The Supporting Information is available free of charge at https://pubs.acs.org/doi/10.1021/acs.macromol.0c02500.

Monomer density profile; raw data of the composite relaxation time; self-intermediate scattering function of different types of chains; and scaled relaxation time of different types of chains (PDF)

■ AUTHOR INFORMATION

Corresponding Author

Francis W. Starr − *Department of Physics, Wesleyan University, Middletown, Connecticut 06459, United States;* orcid.org/0000-0002-2895-6595; Email: fstarr@wesleyan.edu

Authors

Ari Y. Liu − *Department of Physics, Wesleyan University, Middletown, Connecticut 06459, United States;* orcid.org/0000-0002-1582-7292

Hamed Emamy − *Department of Physics, Wesleyan University, Middletown, Connecticut 06459, United States; Department of Chemical Engineering, Columbia University, New York 10027, United States;* orcid.org/0000-0002-5078-5569

Jack F. Douglas − *Materials Science and Engineering Division, National Institute of Standards and Technology, Gaithersburg, Maryland 20899, United States;* orcid.org/0000-0001-7290-2300

Complete contact information is available at: https://pubs.acs.org/10.1021/acs.macromol.0c02500

Notes

The authors declare no competing financial interest.

■ ACKNOWLEDGMENTS

Computer time was provided by Wesleyan University. This work was supported, in part, by NIST Award no. 70NANB19H137.

■ REFERENCES

(1) Koo, J. H. *Fundamentals, Properties, and Applications of Polymer Nanocomposites*; Cambridge University Press, 2016; pp 550−565.

(2) Gangopadhyay, R.; De, A. Conducting polymer nanocomposites: a brief overview. *Chem. Mater.* **2000**, *12*, 608−622.

(3) Balazs, A. C.; Emrick, T.; Russell, T. P. Nanoparticle polymer composites: where two small worlds meet. *Science* **2006**, *314*, 1107−1110.

(4) Schmidt, G.; Malwitz, M. M. Properties of polymer−nanoparticle composites. *Curr. Opin. Colloid Interface Sci.* **2003**, *8*, 103−108.

(5) Moll, J. F.; Akcora, P.; Rungta, A.; Gong, S.; Colby, R. H.; Benicewicz, B. C.; Kumar, S. K. Mechanical reinforcement in polymer melts filled with polymer grafted nanoparticles. *Macromolecules* **2011**, *44*, 7473−7477.

(6) Jordan, J.; Jacob, K. I.; Tannenbaum, R.; Sharaf, M. A.; Jasiuk, I. Experimental trends in polymer nanocomposites−a review. *Mater. Sci. Eng., A* **2005**, *393*, 1−11.

(7) Jancar, J.; Douglas, J. F.; Starr, F. W.; Kumar, S. K.; Cassagnau, P.; Lesser, A. J.; Sternstein, S. S.; Buehler, M. J. Current issues in research on structure−property relationships in polymer nanocomposites. *Polymer* **2010**, *51*, 3321−3343.

(8) Caseri, W. Nanocomposites of polymers and metals or semiconductors: historical background and optical properties. *Macromol. Rapid Commun.* **2000**, *21*, 705−722.

(9) Sanada, K.; Tada, Y.; Shindo, Y. Thermal conductivity of polymer composites with close-packed structure of nano and micro fillers. *Composites, Part A* **2009**, *40*, 724−730.

(10) Cho, J.; Joshi, M. S.; Sun, C. T. Effect of inclusion size on mechanical properties of polymeric composites with micro and nano particles. *Compos. Sci. Technol.* **2006**, *66*, 1941−1952.
(11) Gacitua, E. W.; Ballerini, A. A.; Zhang, J. Polymer nanocomposites: synthetic and natural fillers a review. *Maderas: Cienc. Tecnol.* **2005**, *7*, 159−178.
(12) Wolf, C.; Angellier-Coussy, H.; Gontard, N.; Doghieri, F.; Guillard, V. How the shape of fillers affects the barrier properties of polymer/non-porous particles nanocomposites: A review. *J. Membr. Sci.* **2018**, *556*, 393−418.
(13) Bailey, E. J.; Winey, K. I. Dynamics of polymer segments, polymer chains, and nanoparticles in polymer nanocomposite melts: A review. *Prog. Polym. Sci.* **2020**, *105*, 101242.
(14) Abbasi, H.; Antunes, M.; Velasco, J. I. Recent advances in carbon-based polymer nanocomposites for electromagnetic interference shielding. *Prog. Mater. Sci.* **2019**, *103*, 319−373.
(15) Kumar, A.; Sharma, K.; Dixit, A. R. A review on the mechanical and thermal properties of graphene and graphene-based polymer nanocomposites: understanding of modelling and MD simulation. *Mol. Simul.* **2020**, *46*, 136−154.
(16) Qin, X.; Xia, W.; Sinko, R.; Keten, S. Tuning Glass Transition in Polymer Nanocomposites with Functionalized Cellulose Nanocrystals through Nanoconfinement. *Nano Lett.* **2015**, *15*, 6738−6744.
(17) Karimi, M.; Ghajar, R.; Montazeri, A. A novel interface-treated micromechanics approach for accurate and efficient modeling of CNT/polymer composites. *Compos. Struct.* **2018**, *201*, 528−539.
(18) Kumar, S. K.; Benicewicz, B. C.; Vaia, R. A.; Winey, K. I. 50th Anniversary Perspective: Are Polymer Nanocomposites Practical for Applications? *Macromolecules* **2017**, *50*, 714−731.
(19) Starr, F. W.; Schrøder, T. B.; Glotzer, S. C. Molecular Dynamics Simulation of a Polymer Melt with a Nanoscopic Particle. *Macromolecules* **2002**, *35*, 4481−4492.
(20) Starr, F. W.; Schrøder, T. B.; Glotzer, S. C. Effects of a nanoscopic filler on the structure and dynamics of a simulated polymer melt and the relationship to ultrathin films. *Phys. Rev. E: Stat., Nonlinear, Soft Matter Phys.* **2001**, *64*, 021802.
(21) Starr, F. W.; Douglas, J. F.; Glotzer, S. C. Origin of particle clustering in a simulated polymer nanocomposite and its impact on rheology. *J. Chem. Phys.* **2003**, *119*, 1777−1788.
(22) Pazmiño Betancourt, B. A.; Douglas, J. F.; Starr, F. W. Fragility and cooperative motion in a glass-forming polymer-nanoparticle composite. *Soft Matter* **2013**, *9*, 241−254.
(23) Ma, P.-C.; Siddiqui, N. A.; Marom, G.; Kim, J.-K. Dispersion and functionalization of carbon nanotubes for polymer-based nanocomposites: A review. *Composites, Part A* **2010**, *41*, 1345−1367.
(24) Hooper, J. B.; Schweizer, K. S. Contact Aggregation, Bridging, and Steric Stabilization in Dense Polymer-Particle Mixtures. *Macromolecules* **2005**, *38*, 8858−8869.
(25) Rittigstein, P.; Priestley, R. D.; Broadbelt, L. J.; Torkelson, J. M. Model polymer nanocomposites provide an understanding of confinement effects in real nanocomposites. *Nat. Mater.* **2007**, *6*, 278−282.
(26) Kropka, J. M.; Pryamitsyn, V.; Ganesan, V. Relation between Glass Transition Temperatures in Polymer Nanocomposites and Polymer Thin Films. *Phys. Rev. Lett.* **2008**, *101*, 075702.
(27) Priestley, R. D.; Cangialosi, D.; Napolitano, S. On the equivalence between the thermodynamic and dynamic measurements of the glass transition in confined polymers. *J. Non-Cryst. Solids* **2015**, *407*, 288−295.
(28) Holt, A. P.; Griffin, P. J.; Bocharova, V.; Agapov, A. L.; Imel, A. E.; Dadmun, M. D.; Sangoro, J. R.; Sokolov, A. P. Dynamics at the Polymer/Nanoparticle Interface in Poly(2-vinylpyridine)/Silica Nanocomposites. *Macromolecules* **2014**, *47*, 1837−1843.
(29) Holt, A. P.; Sangoro, J. R.; Wang, Y.; Agapov, A. L.; Sokolov, A. P. Chain and Segmental Dynamics of Poly(2-vinylpyridine) Nanocomposites. *Macromolecules* **2013**, *46*, 4168−4173.
(30) Harton, S. E.; Kumar, S. K.; Yang, H.; Koga, T.; Hicks, K.; Lee, H.; Mijovic, J.; Liu, M.; Vallery, R. S.; Gidley, D. W. Immobilized Polymer Layers on Spherical Nanoparticles. *Macromolecules* **2010**, *43*, 3415−3421.
(31) Starr, F. W.; Douglas, J. F.; Meng, D.; Kumar, S. K. Bound Layers "Cloak" Nanoparticles in Strongly Interacting Polymer Nanocomposites. *ACS Nano* **2016**, *10*, 10960−10965.
(32) Emamy, H.; Kumar, S. K.; Starr, F. W. Diminishing Interfacial Effects with Decreasing Nanoparticle Size in Polymer-Nanoparticle Composites. *Phys. Rev. Lett.* **2018**, *121*, 207801.
(33) Moll, J.; Kumar, S. K. Glass Transitions in Highly Attractive Highly Filled Polymer Nanocomposites. *Macromolecules* **2012**, *45*, 1131−1135.
(34) Zhang, W.; Douglas, J. F.; Starr, F. W. Why we need to look beyond the glass transition temperature to characterize the dynamics of thin supported polymer films. *Proc. Natl. Acad. Sci. U.S.A.* **2018**, *115*, 5641−5646.
(35) Emamy, H.; Kumar, S. K.; Starr, F. W. Structural Properties of Bound Layer in Polymer−Nanoparticle Composites. *Macromolecules* **2020**, *53*, 7845−7850.
(36) Tsagaropoulos, G.; Eisenberg, A. Dynamic Mechanical Study of the Factors Affecting the Two Glass Transition Behavior of Filled Polymers. Similarities and Differences with Random Ionomers. *Macromolecules* **1995**, *28*, 6067−6077.
(37) Akcora, P.; Kumar, S. K.; García Sakai, V.; Li, Y.; Benicewicz, B. C.; Schadler, L. S. Segmental Dynamics in PMMA-Grafted Nanoparticle Composites. *Macromolecules* **2010**, *43*, 8275−8281.
(38) Hall, L. M.; Schweizer, K. S. Many body effects on the phase separation and structure of dense polymer-particle melts. *J. Chem. Phys.* **2008**, *128*, 234901.
(39) Lin, E. Y.; Frischknecht, A. L.; Riggleman, R. A. Origin of Mechanical Enhancement in Polymer Nanoparticle (NP) Composites with Ultrahigh NP Loading. *Macromolecules* **2020**, *53*, 2976−2982.
(40) Surve, M.; Pryamitsyn, V.; Ganesan, V. Polymer-bridged gels of nanoparticles in solutions of adsorbing polymers. *J. Chem. Phys.* **2006**, *125*, 064903.
(41) Senses, E.; Tyagi, M.; Natarajan, B.; Narayanan, S.; Faraone, A. Chain dynamics and nanoparticle motion in attractive polymer nanocomposites subjected to large deformations. *Soft Matter* **2017**, *13*, 7922−7929.
(42) Sorichetti, V.; Hugouvieux, V.; Kob, W. Structure and Dynamics of a Polymer−Nanoparticle Composite: Effect of Nanoparticle Size and Volume Fraction. *Macromolecules* **2018**, *51*, 5375−5391.
(43) Hanakata, P. Z.; Douglas, J. F.; Starr, F. W. Local variation of fragility and glass transition temperature of ultra-thin supported polymer films. *J. Chem. Phys.* **2012**, *137*, 244901.
(44) Starr, F. W.; Douglas, J. F. Modifying Fragility and Collective Motion in Polymer Melts with Nanoparticles. *Phys. Rev. Lett.* **2011**, *106*, 115702.
(45) Zhang, W.; Emamy, H.; Pazmiño Betancourt, B. A.; Vargas-Lara, F.; Starr, F. W.; Douglas, J. F. The interfacial zone in thin polymer films and around nanoparticles in polymer nanocomposites. *J. Chem. Phys.* **2019**, *151*, 124705.
(46) O'Driscoll, K.; Sanayei, R. A. Chain-length dependence of the glass transition temperature. *Macromolecules* **1991**, *24*, 4479−4480.
(47) Thompson, E. V. Dependence of the glass transition temperature of poly(methyl methacrylate) on tacticity and molecular weight. *J. Polym. Sci.* **1966**, *4*, 199−208.
(48) Schnell, B.; Meyer, H.; Fond, C.; Wittmer, J. P.; Baschnagel, J. Simulated glass-forming polymer melts: Glass transition temperature and elastic constants of the glassy state. *Eur. Phys. J. E: Soft Matter Biol. Phys.* **2011**, *34*, 97.
(49) Lobe, B.; Baschnagel, J. Monte Carlo simulation of the glass transition in two- and three-dimensional polymer melts: Influence of the spatial dimension. *J. Chem. Phys.* **1994**, *101*, 1616−1624.
(50) Fox, T. G.; Flory, P. J. Second-Order Transition Temperatures and Related Properties of Polystyrene. I. Influence of Molecular Weight. *J. Appl. Phys.* **1950**, *21*, 581−591.

https://doi.org/10.1021/acs.macromol.0c02500
Macromolecules 2021, 54, 3041−3051

(51) Fox, T. G.; Flory, P. J. The glass temperature and related properties of polystyrene. Influence of molecular weight. *J. Polym. Sci.* **1954**, *14*, 315−319.
(52) Plimpton, S. Fast Parallel Algorithms for Short-Range Molecular Dynamics. *J. Comput. Phys.* **1995**, *117*, 1−19.
(53) Crawford, M.; Smalley, R.; Cohen, G.; Hogan, B.; Wood, B.; Kumar, S.; Melnichenko, Y. B.; He, L.; Guise, W.; Hammouda, B. Chain conformation in polymer nanocomposites with uniformly dispersed nanoparticles. *Phys. Rev. Lett.* **2013**, *110*, 196001.
(54) Doxastakis, M.; Chen, Y.-L.; Guzmán, O.; de Pablo, J. J. Polymer−particle mixtures: Depletion and packing effects. *J. Chem. Phys.* **2004**, *120*, 9335−9342.
(55) Frischknecht, A. L.; McGarrity, E. S.; Mackay, M. E. Expanded chain dimensions in polymer melts with nanoparticle fillers. *J. Chem. Phys.* **2010**, *132*, 204901.
(56) Green, P. F. The structure of chain end-grafted nanoparticle/homopolymer nanocomposites. *Soft Matter* **2011**, *7*, 7914−7926.
(57) Karatrantos, A.; Clarke, N.; Composto, R. J.; Winey, K. I. Polymer conformations in polymer nanocomposites containing spherical nanoparticles. *Soft Matter* **2015**, *11*, 382−388.
(58) Liu, J.; Wu, Y.; Shen, J.; Gao, Y.; Zhang, L.; Cao, D. Polymer−nanoparticle interfacial behavior revisited: A molecular dynamics study. *Phys. Chem. Chem. Phys.* **2011**, *13*, 13058−13069.
(59) Picu, R. C.; Ozmusul, M. S. Structure of linear polymeric chains confined between impenetrable spherical walls. *J. Chem. Phys.* **2003**, *118*, 11239−11248.
(60) Ozmusul, M. S.; Picu, R. C. Structure of polymers in the vicinity of convex impenetrable surfaces: the athermal case. *Polymer* **2002**, *43*, 4657−4665.
(61) Sen, S.; Xie, Y.; Kumar, S. K.; Yang, H.; Bansal, A.; Ho, D. L.; Hall, L.; Hooper, J. B.; Schweizer, K. S. Chain Conformations and Bound-Layer Correlations in Polymer Nanocomposites. *Phys. Rev. Lett.* **2007**, *98*, 128302.
(62) Bhadauriya, S.; Wang, X.; Nallapaneni, A.; Masud, A.; Wang, Z.; Lee, J.; Bockstaller, M. R.; Al-Enizi, A. M.; Camp, C. H., Jr.; Stafford, C. M.; Douglas, J. F.; Karim, A. Observation of General Entropy-Enthalpy Compensation Effect in the Relaxation of Wrinkled Polymer Nanocomposite Films. *Nano Lett.* **2021**, *21*, 1274. , in press
(63) Mangalara, J. H.; Simmons, D. S. Tuning Polymer Glass Formation Behavior and Mechanical Properties with Oligomeric Diluents of Varying Stiffness. *ACS Macro Lett.* **2015**, *4*, 1134−1138.
(64) Bormuth, A.; Henritzi, P.; Vogel, M. Chain-Length Dependence of the Segmental Relaxation in Polymer Melts: Molecular Dynamics Simulation Studies on Poly(propylene oxide). *Macromolecules* **2010**, *43*, 8985−8992.
(65) Dobkowski, Z. Influence of molecular weight distribution and long chain branching on the glass transition temperature of polycarbonate. *Eur. Polym. J.* **1982**, *18*, 563−567.
(66) Chremos, A.; Douglas, J. F. Communication: When does a branched polymer become a particle? *J. Chem. Phys.* **2015**, *143*, 111104.

https://doi.org/10.1021/acs.macromol.0c02500
Macromolecules 2021, 54, 3041−3051